

Interactive comment on “Daytime aerosol optical depth above low-level clouds is similar to that in adjacent clear skies at the same heights: airborne observation above the southeast Atlantic” by Yohei Shinozuka et al.

Yohei Shinozuka et al.

yohei.shinozuka@nasa.gov

Received and published: 15 June 2020

Eric Wilcox (Referee)

We would like to thank Dr. Wilcox for the review.

This paper provides a valuable check on a frequent assumption in aerosol cloud studies: that aerosol properties, including optical thickness and intrinsic properties, such as particle optical properties, in cloudy skies are similar to those same properties in the clear-sky areas between clouds. This assumption is made in a large segment of

C1

the literature using passive remote sensing data of aerosols and clouds to investigate possible effects of aerosols on clouds, such as microphysical or radiative effects. In particular, the paper focuses on the southeast Atlantic Ocean case where light absorbing smoke resides above stratocumulus clouds. In doing so, they also provide a more detailed commentary on our previous paper (Chung et al. 2016), which found a curious difference in aerosol optical thickness (AOT) above cloud compared to clear air near clouds in CALIOP data that is different for daytime overpasses than for nighttime overpasses. This new paper is a useful application of recent high-quality airborne measurements to revisit these issues and is a valuable contribution. I recommend some revisions based on the following comments.

While the authors find no statistically significant difference in AOT above cloud compared to the adjacent cloud-free region, they do find a significant difference in the particle number concentration under the mesoscale averaging method, which combines observations from within 2 degree lat/lon boxes. This result is at odds with the finer scale analysis of the same quantity. To explain, the authors refer to a criterion on “outliers”, but I think there is room for more discussion. In addition to clarifying what the outlier criterion is, I wonder if the extreme variability of this quantity in airborne measurements of the free troposphere due to layering of aerosol plumes, for example, make it likely that the sampling is insufficient to even address this metric. One way to evaluate this for particle concentration, as well as the other metrics, is to ask the question: given the observed variability is it likely that the number of samples present is sufficient to adequately sample clear and cloudy air within the 2 deg. box at all? Given that analysis of cloudy air to adjacent clear air shows no significant difference, I suspect that the real problem here is that you have not adequately measured the average particle concentration in the box. This question should probably be evaluated for particle concentration and the other metrics under the meso-scale sampling method.

We agree. We have modified the sampling method to reduce the error. We exclude the boxes with fewer than 10 samples, as noted now in Section 2.2. Note that the new

C2

restriction has reduced the sample data volume only by 5 minutes or less, depending on aerosol property.

The particle number concentration no longer shows a low p value, no longer at odds with the fine scale analysis. The original second paragraph of the results section that described the anomaly has been removed. We have updated the first paragraph and Figure 4 for AODct and Table 2 for all other aerosol properties as well. The results section now points out “The only exception [to the high p values] is the organic mass with a p value just under 0.05 (before rounding).”

While the modification mitigates the error in representing the boxes, the fundamental limitation remains: The airborne data are not optimized for statistical analysis in the meso-scale monthly-mean. We nonetheless employ this scale to provide the best possible reference point for satellite-based analysis, as stated in Section 2. In parallel, we present the local-scale near-synchronous sampling method to best exploit the spatiotemporal resolution of the airborne data.

On the matter of reconciling these new results with the previous Chung et al. (2016) paper, I recommend clarifying a couple of points:

(1) One of the pieces of evidence that the differences between above cloud and clearair AOT might be an artifact of the CALIOP data is the contrast between the daytime and nighttime difference. This is emphasized by Chung et al. where they note that “The global average AODct above low clouds is much larger during the nighttime than during the daytime for all seasons (Table 1), which is most likely related to a higher S/N [signal-to-noise ratio] for nighttime retrievals compared to those during the daytime” (p. 5788) and again on p. 5790. While the submitted manuscript mentions that detecting aerosol layers is sensitive to the signal-to-noise ratio which is impacted by the background lighting conditions (lines 67 and 304), it does not clearly make the point that this leads to a strong day/night contrast in the detectability limit. This is, of course, well known in the remote sensing community, but I think that the paper could make this part of the

C3

work more accessible to a broader readership by expressing this simple point more directly.

We agree. The discussion now says ‘As described in Sect. 1, the CALIOP standard algorithm has a detection bias that leads to greater AOD underestimates over clouds than in clear skies due to upward sunlight reflection. The authors [Chung et al. (2016)] emphasize that this bias might explain their results, pointing to a day-night contrast as evidence: “a corresponding difference cannot be seen in the Δ AODct derived from nighttime retrievals [which are free of sunlight reflection]”. We have chosen the quote on Δ AODct instead of AODct, to address not only the day-night contrast but also its implications on the cloudy-clear contrast. We have also revised the fourth paragraph of the introduction to emphasize the findings by Chung et al. (2016), with the quote “might simply be a result of systematic differences between the detection thresholds in clear sky and above low bright clouds.”

(2) The paper uses data from HSRL and finds no evidence of the differences between above-cloud and clear-air AOT reported in the Chung et al (2016) paper, and builds further support that the differences reported in Chung et al. (2016) are an artifact of the CALIOP data. However, on line 73 the authors also note that Kacenelenbogen et al. (2014) “saw no clear bias” in above cloud AOD between CALIOP and HSRL. How are we to reconcile these two points that seem contradictory?

As described in Kacenelenbogen et al. (2014), an error in the daytime CALIOP standard AOD product mainly originates from either (i) a misclassified aerosol type (and hence, a wrongly assumed lidar ratio in the CALIOP algorithm) and/ or (ii) a low SNR (especially when solar light is reflected on the underlying cloud). Factor (i) will either over or underestimate CALIOP AOD whereas factor (ii) will lead to undetected aerosol layers above clouds (i.e. the underestimation of the aerosol geometrical thickness) and an underestimation of the CALIOP AOD.

In Chung et al. (2016), the authors compare CALIOP standard AOD products in clear

C4

skies and above near-by clouds. The lower daytime CALIOP AOD above clouds can be explained mainly by factor (ii), as there is no reason to assume a different aerosol classification bias (i.e., factor i) in both clear skies and above near-by clouds.

Kacenenbogen et al. (2014) saw no clear bias in above cloud AOD between CALIOP and HSRL due to the fact that both factors (i) and (ii) are at play and also, possibly, that the study is based on low AAC AOD values (limited number of coincident HSRL-CALIOP AAC cases over Northern America with a majority of AAC AOD < 0.1 and average HSRL AAC AOD of 0.04 ± 0.05). On the other hand, and similar to the results in Chung et al. (2016), Liu et al. (2015) describe a CALIOP standard daytime AOD underestimation above clouds over two regions of high AAC AOD values (i.e., Saharan dust across the Atlantic and Smoke in the South East Atlantic). In Liu et al., (2015), while both factors (i) and (ii) are also at play, they mainly explain the CALIOP AAC AOD underestimation by factor (ii) in the South East Atlantic, and by factor (i) in the case of Saharan dust (see their Table 2).

We have inserted the explanations in the discussion section.

We have made several voluntary changes. The buffer below the P-3 is now described as "a certain depth, 1500 m for most flights" instead of 1500 m. Fig. 3c, originally of a 2018 flight, has been replaced with a 2017 flight. The word environment is now treated as countable. A small number of phrases such as "Going back to the present aircraft-based study" have been inserted for a better flow. See also the other review and our response to it.

Anonymous Referee 2

We would like to thank Anonymous Referee 2 for the review.

This paper uses recent airborne high-spectral-resolution lidar (HSRL) and sunphotometer observations to examine an assumption that aerosol properties over low clouds are similar to that in the neighboring clear sky. This assumption is widely used in the

C5

studies that investigate aerosol radiative effects in cloudy and clear-sky conditions using passive satellite remote sensing data. The paper referenced a previous study by Chung et al that used the satellite-borne CALIOP observation to examine the aerosol optical depth (AOD) difference in cloudy and clear-sky conditions. The Chung et al paper revealed a large day and night difference that is most likely related to the CALIOP measurement. CALIOP is an active lidar instrument and can provide globally range-resolved cloud and aerosol vertical profiles. Its return signal is generally weak due to the high altitude (>700 km) of the satellite orbit, and the data SNR for daytime is not as good as that during nighttime in the presence of large sunlight background noise. Therefore, some tenuous aerosol layers can be missed in the feature detection. This can cause underestimate of daytime AOD. The airborne HSRL measurement used in this study has much larger SNR than that of the CALIOP measurement and can provide the aerosol extinction as well as lidar ratio which is modeled in the CALIOP data processing. This paper uses this HSRL dataset to revisit the cloudy and clear-sky AOD difference. The study is very useful and valuable. I suggest the paper published after some revision.

In the paper, the authors concluded that daytime 532 nm AOD over low-level clouds is similar to that in the surrounding clear skies at the same heights. This supports the assumption mentioned above in the geographical region and season investigated. However, some information and analysis results presented in the paper are confusing and need more explanation and clarification. My biggest confusion is with the statistical analysis using t-test in the paper. In figure 6, the mean 532 nm AODct difference approaches zero as the separation distance between the aerosol layer over cloud and in the surrounding clear sky decreases. This is as I expect. However, the p-values from the t-test are smaller than the threshold of 0.05 for smaller separation distances, suggesting that the null hypothesis of zero AODct difference is rejected (refer to lines 227-228) at a confidence level of 95

True, the null hypothesis is rejected for this subset of the statistical analysis. The small

C6

p-values and large t-values are explained by the small standard error, which in turn results from the small standard deviation and the large sample number.

Our discussion, nonetheless, puts little emphasis on this subset of analysis, because of sampling ambiguity and practical insignificance. First, the transition of aerosols to activated droplets in the so-called twilight zone makes the definition of clear and cloudy sides ambiguous. Second, the mean AOD difference as close to zero as -0.002 has little practical significance to climate science, notwithstanding its statistical significance relative to the standard error.

The manuscript now clarifies “[...] most of which, with minimum separation of 0-2 km, are subject to potential ambiguity associated with the so-called twilight zone (Sect. 2.2.2).” “Given that a p-value of 0.05 simply means that there is a one in 20 chance that the null hypothesis is correct, we expect some low p-values just by chance as we conduct many comparisons.”

Some minor comments:

It may be useful to provide the expression of t-test that can help the discussion and interpretation about the results.

A mathematical expression has been inserted in Section 2.3.

The mean difference is compared to RMSD (line 241, line 249 and line 255) in the discussion about the results in this paper. It may make more sense to compare the mean difference and standard deviation (or RMSD) to the corresponding mean value of each parameter.

True. Table 2 now has a column for the mean value. The result section and Figure 4 refer to this.

In Table 2, statistics of log₁₀532 nm AOD_{ct} difference are listed, in addition to 532 nm AOD_{ct} difference. Is there a reason for this? Any additional information can be drawn from it? A little bit more explanation is needed.

C7

Both linear and logarithmic scales are common when plotting AOD. We just wanted to reassure that our conclusions hold regardless of scale. We have added “something we tested just to confirm that our conclusions do not depend on the choice of linear or log scale”,

We have made several voluntary changes. The buffer below the P-3 is now described as “a certain depth, 1500 m for most flights” instead of 1500 m. Fig. 3c, originally of a 2018 flight, has been replaced with a 2017 flight. The word environment is now treated as countable. A small number of phrases such as “Going back to the present aircraft-based study” have been inserted for a better flow. See also the other review and our response to it.

Interactive comment on Atmos. Chem. Phys. Discuss., <https://doi.org/10.5194/acp-2019-1007>, 2020.

C8

1 **Daytime aerosol optical depth above low-level**
2 **clouds is similar to that in adjacent clear skies**
3 **at the same heights: airborne observation**
4 **above the southeast Atlantic**

5 Yohei Shinozuka^{1,2}, Meloë S. Kacenelenbogen², Sharon P. Burton³, Steven G. Howell⁴, Paquita
6 Zuidema⁵, Richard A. Ferrare³, Samuel E. LeBlanc^{2,6}, Kristina Pistone^{2,6}, Stephen Broccardo^{1,2},
7 Jens Redemann⁷, K. Sebastian Schmidt⁸, Sabrina P. Cochrane^{8,9}, Marta Fenn^{3,10}, Steffen Freitag⁴,
8 Amie Dobracki^{4,5}, Michal Segal-Rosenheimer^{2,6,11}, Connor J. Flynn⁷

9
10 ¹ Universities Space Research Association, Columbia, Maryland, USA

11 ² NASA Ames Research Center, Moffett Field, California, USA

12 ³ NASA Langley Research Center, Hampton, Virginia, USA

13 ⁴ University of Hawaii at Manoa, Honolulu, Hawaii, USA

14 ⁵ University of Miami, Miami, Florida, USA

15 ⁶ Bay Area Environmental Research Institute, Moffett Field, California, USA

16 ⁷ University of Oklahoma, Norman, Oklahoma, USA

17 ⁸ University of Colorado, Boulder, Colorado, USA

18 ⁹ Laboratory for Atmospheric and Space Physics, Boulder, Colorado, USA

19 ¹⁰ Science Systems and Applications, Inc, Hampton, VA, USA

20 ¹¹ Department of Geophysics, Porter School of the Environment and Earth Sciences, Tel-Aviv
21 University, Tel-Aviv, Israel

22 *Correspondence to:* Y. Shinozuka (Yohei.Shinozuka@nasa.gov)

23 **Abstract**

24 To help satellite retrieval of aerosols and studies of their radiative effects, we demonstrate
25 that daytime ~~532 nm~~-aerosol optical depth over low-level clouds is similar to that in neighboring
26 clear skies at the same heights ~~in~~. Based on recent airborne lidar and sunphotometer observations
27 above the southeast Atlantic. ~~The, the~~ mean AOD difference at 532 nm is between 0 and -0.01,
28 when comparing the cloudy and clear sides, each up to 20 km wide, of cloud edges. The difference
29 is not statistically significant according to a paired t-test. Systematic differences in the wavelength
30 dependence of AOD and in situ single scattering albedo are also ~~minute~~minuscule. These results
31 hold regardless of the vertical distance between cloud top and aerosol layer bottom. AOD
32 aggregated over $\sim 2^\circ$ grid boxes for each of September 2016, August 2017 and October 2018 also
33 shows little correlation with the presence of low-level clouds. We posit that a satellite retrieval
34 artifact is entirely responsible for a previous finding of generally smaller AOD over clouds (Chung
35 et al., 2016), at least for the region and time of our study. Our results also suggest that the same
36 values can be assumed for the intensive properties of free-tropospheric biomass-burning aerosol
37 regardless of whether clouds ~~exist~~are present below.

38 **1. Introduction**

39 A significant amount of atmospheric particles are transported above liquid water clouds on
40 the global scale (Waquet et al., 2013). Aerosols above clouds (AAC) may influence the climate in
41 three ways. ~~Their; their~~ light absorption ~~is~~may be amplified by cloud reflection. ~~The; the~~ heating
42 of the atmosphere due to the absorption may stabilize the atmosphere. ~~The; and the~~ particles may
43 eventually subside, enter the underlying clouds and alter their properties. Estimates of the direct
44 aerosol radiative effect alone see large inter-model spread for areas with large aerosol optical depth
45 (AOD) over widespread clouds (Stier et al., 2013; Zuidema et al., 2016).

46 Since AAC are difficult to see from the ground or a ship, previous studies have relied on
47 satellite observations (see Table 1 and 2 of (Kacenelenbogen et al. see Table 2 of
48 (2019)Kacenelenbogen et al., 2019).). Among them is Chung et al. (2016), which used the level 2
49 products of the Cloud-Aerosol Lidar with Orthogonal Polarization (CALIOP) (Winker et al., 2009)
50 to calculate the AOD above the maximum low-cloud-top-height in each grid cell in clear sky as
51 well as the AOD above low clouds on a global $2^\circ \times 5^\circ$ latitude–longitude grid. Their results indicate

52 that daytime 532 nm AOD above low clouds is generally lower than that in clear sky at the same
53 heights. The difference is up to 0.04 over the southeastern Atlantic Ocean (see their Fig. 2)).

54 As Chung et al. (2016) point out, it is conceivable that aerosol amounts over cloud can be
55 different from those in nearby clear sky. There are two sets of potential reasons. The first concerns
56 the effects of meteorology. Large-scale circulation patterns paired with solar reflection from clouds
57 on aerosols could modify the horizontal and vertical extent of aerosols, aerosol concentration and
58 chemical composition. For example, the properties of hygroscopic aerosols might vary if the
59 relative humidity in clear skies is somehow higher than above clouds. The second set of reasons
60 pertain to the case of aerosols in close proximity to clouds. ~~The~~That proximity has been variously
61 defined, for example less than 100 m in the vertical direction (Costantino and Bréon, 2013) and
62 less than 20 km in the horizontal direction (Várnai and Marshak, 2018). Chung et al. (2016) note
63 that aerosols were shown to influence underlying cloud by indirect effects and semidirect effects
64 (Costantino and Bréon, 2010, 2013; Johnson et al., 2004; Wilcox, 2010) and that these aerosol-
65 cloud interactions and possibly more ~~(e.g., a pronounced if unlikely aerosol entrainment (Diamond
66 et al., 2018))~~ might somehow affect the aerosol amount over cloud. ~~A bias in the CALIOP standard
67 retrieval was also raised as a possible explanation for the~~

68 Chung et al. (2016) ~~results raise a bias in the CALIOP standard retrieval as another possible
69 explanation. The retrieval algorithm confines itself to distinct aerosol layers whose signals are high
70 enough compared to detector noise.~~ The detection threshold ~~in the feature detection algorithm~~
71 varies ~~depending on the background lighting conditions,~~with the atmospheric features (e.g.,
72 aerosols, high altitude cirrus or boundary layer clouds) ~~and~~, the horizontal averaging required by
73 CALIOP for detection and, importantly, the background lighting conditions (see Fig. 4 of Winker
74 et al. (2009)). ~~In the particular case of aerosols above clouds, Kacenelenbogen et al. (2014) show
75 that the CALIOP standard algorithm substantially underestimates the frequency of AAC when the
76 AOD is less than ~0.02. This is due mostly to tenuous aerosols with a backscatter under the
77 detection threshold; however, Kacenelenbogen et al. (2014) saw no clear bias in AOD above
78 clouds between CALIOP and the NASA Langley airborne High Spectral Resolution Lidar (HSRL-
79 1). Liu et al. (2015) show a clear AOD underestimate of the CALIOP level 2 retrieval in
80 comparison to a separate retrieval after Hu et al. (2007) for smoke above opaque water clouds over
81 the southeast Atlantic, and explain this by the CALIOP layer detection scheme prematurely
82 assigning layer base altitudes and thus underestimating the geometric thickness of smoke layers.~~

83 ~~According to Chung et al. (2016), the negative daytime AOD differences between cloudy and~~
84 ~~cloud-free conditions~~If the signal-to-noise (S/N) ratio of a layer is not high enough, no extinction
85 is reported for the portion of the aerosol profile; summing up the extinction produces a low-biased
86 AOD. Because the upward sunlight reflection adds to the background noise, the AOD
87 underestimate is likely more pronounced above clouds than in clear skies. Chung et al. (2016) state
88 that their results “might simply be a result of systematic differences between the detection
89 thresholds in clear sky and above low bright clouds”. ~~The authors add that the bias may be~~
90 ~~enhanced over the ocean due to the lower albedo compared to that of land.”~~ Layer detection and
91 other sources of uncertainty in the CALIPSO standard algorithm are also discussed by
92 Kacenelenbogen et al. (2014) and Liu et al. (2015).

93 The subject warrants further investigation, given the importance of AAC on climate. An
94 airborne experiment can help by providing direct measurements that are subject to smaller
95 uncertainty, in with finer spatial and temporal resolution albeit over limited ranges. The NASA
96 ObseRvations of Aerosols above CLouds and their intEractionS (ORACLES) mission was carried
97 out to study key processes that determine the climate impacts of African biomass-burning aerosols
98 above the southeast Atlantic. Of the two deployed aircraft, the NASA P3, equipped with in situ
99 and remote sensing instruments, flew in the lower- to mid-troposphere, mostly in September 2016,
100 August 2017 and October 2018. In September 2016 the NASA ER2 also flew, at about 20 km
101 altitude with downward-viewing sensors. Extensive stratocumulus clouds were observed
102 repeatedly throughout the mission; see a sample satellite image in ~~Redemann et al. (in~~
103 ~~preparation)~~Sayer et al. (2019). Details of the ORACLES mission can be found in Redemann et
104 al. (in preparation2020), Zuidema et al. (2016) and Shinozuka et al. (2019).

105 The instrumentation relevant to the present paper is described in Sect. 2 along with
106 sampling and statistical hypothesis testing methods. This is followed by comparisons of AOD and
107 other aerosols properties above the height of cloud top between cloudy and clear skies (Sect. 3).
108 Sect. 4 offers discussion.

2. Methods

2.1. Instrumentation

The remote sensing and in situ instruments used in this study are briefly described below with references to full descriptions. Note that the measurements each refer to a unique vertical range, as summarized in Table 1.

The NASA Langley Research Center High Spectral Resolution Lidar (HSRL-2), deployed from the ER2 in 2016 and from the P3 in 2017 and 2018, measures calibrated, unattenuated backscatter and aerosol extinction profiles below the instrument. The data are reported with 10 s intervals. The HSRL-2 ~~signal-to-noise~~S/N ratio is higher than that of CALIOP, due to the much lower altitude and the inverse square dependence of light intensity. In addition, by the use of a second channel to assess aerosol attenuation, the HSRL technique (Shipley et al., 1983) results in an accurate aerosol extinction product with no assumptions about lidar ratio, and also a more accurate backscatter product, particularly in the lower atmosphere where attenuation by upper layers can present difficulties for the spaceborne backscatter lidar. Differences in algorithm are discussed in Sect. 4. Further details about the instrument, calibration and uncertainty can be found in Hair et al. (2008), Rogers et al. (2009) and Burton et al. (2018).

Our analysis utilizes the HSRL-2 standard products of cloud top height (CTH), 532 nm particulate backscattering and 532 nm aerosol optical thickness (Burton et al., 2012) in three ways. First, flight segments are isolated using the CTH product (detailed in Sect. 2.2). Second, the bottom and top heights of the smoke plumes are defined with a (somewhat arbitrarily chosen) threshold backscattering coefficient at $0.25 \text{ Mm}^{-1}\text{sr}^{-1}$ after Shinozuka et al. (2019).

Third, we evaluate the 532 nm partial-column aerosol optical thickness from below the aircraft down to ~50 m above the CTH, (even for columns without clouds; see Sect. 2.2). The ~50-m buffer is designed to reduce the ambiguity associated with the transition at the cloud top. The upper limit of the integral of extinction is 14 km altitude for the 2016 ER2 flights and a certain depth, 1500 m for most flights, below the P3 altitude for 2017 and 2018- (Fig. 1). Profiles with possible influences of mid- and high-level clouds are largely excluded from the product, though isolated cases of thin clouds may remain.

We also use partial-column AOD observed upward from the P3 with a sunphotometer- (Fig. 1b,c). The Spectrometer for Sky-Scanning, Sun-Tracking Atmospheric Research (4STAR) measures hyper-spectral direct solar beam. Calculated AOD is reported at 1 Hz. Our analysis

140 excludes data with possible influences of clouds above the instrument. Further details on the
141 instrument as well as data acquisition, screening, calibration and reduction can be found in
142 Dunagan et al. (2013), Shinozuka et al. (2013) and LeBlanc et al. (2019).

143 For 2017 and 2018, we examine a combination of the 4STAR and HSRL-2 AODs, in order
144 to cover the free troposphere both upward and downward from the aircraft that flew in it (Fig.
145 [41b,c](#)). The vertical coverage is compromised by two limitations intrinsic to the lidar
146 measurements. First, the CTH is not sought within 500 m of the instrument (not to be confused
147 with the ~50-m lower buffer for the extinction integral). This means that the flight segments with
148 clouds so close to the aircraft enter our analysis only if the clouds extended as deep as to reach 500
149 m away from it. This is at most a minor fraction of the data, as the fraction with the CTH within
150 550 m of the P3 altitude is a mere 3%. Second, because of the 1500 m upper buffer for the [P3-](#)
151 [borne HSRL-2](#) extinction integral, we only have 4STAR above-P3 AOD for the flight segments
152 when the plane was 500-1500 m above the CTH (Fig. 1b). We add the HSRL-2 AOD to the 4STAR
153 AOD only for the flight segments when the P3 was >1500 m above the CTH (Fig. 1c).

154 For 2016, we examine the [ER2-borne](#) HSRL-2 AOD only, because, with the lidar above
155 the troposphere, two of the missing layers can safely be ignored, leaving the ~50 m lower buffer
156 as the only missing layer (Fig. 1a). We refer to all these AODs from the three campaigns
157 collectively as AOD_{ct} (see Table 1). The wavelength dependence expressed as Angstrom exponent
158 is calculated for 10-s periods with AOD_{ct} at 355 and 532 nm both exceeding 0.1.

159 In situ aerosol instruments operated from the P3 include a nephelometer (TSI model 3563)
160 and a particle soot absorption photometer (PSAP, Radiance Research 3-wavelength version),
161 which measure particulate light scattering and absorption, respectively. After adjustments are
162 made for factors such as angular truncations (Anderson and Ogren, 1998) and filter interference
163 (Virkkula, 2010) for each wavelength, extinction coefficient and single scattering albedo at 550
164 nm are derived for an instrument relative humidity (RH) that is typically below 40%. [See](#) Pistone
165 et al. (2019) and Shinozuka et al. (2019) [havefor](#) more details. The non-refractory masses of
166 submicron particles were measured by a time-of-flight aerosol mass spectrometer (Aerodyne, Inc
167 HR-ToF AMS, DeCarlo et al. (2006)). A condensation particle counter (TSI model 3010, with ΔT
168 set to 22°C) measured the number concentration of particles larger than about 10 nm. These in situ
169 properties refer to the air immediately outside the P3 aircraft, not a vertical column. Only the in

170 situ measurements in 2017 and 2018 at 500-1500 m above the CTH are used in this study. (Fig.
171 [1b](#)).

172 **2.2. Sampling**

173 Two methods are employed for selecting subsets of the observations for analysis. In the
174 first (Sect. 2.2.1), we bundle data from areas hundreds of kilometers wide for each of the three
175 campaigns, in a manner as similar to the CALIOP-based study (Chung et al., 2016) as the airborne
176 measurements allow. In the second method (Sect. 2.2.2), we pair cloudy and clear skies with more
177 stringent spatiotemporal criteria to isolate the impact of finer-scale phenomena. Note that both
178 methods ignore time periods for which the 532 nm backscattering product (from which the CTH
179 product is derived) is masked at all altitudes, as well as transit flights into and out of the study area.
180 Cases are also excluded where the CTH exceeds 3241 m. This is to be consistent with the study
181 by Chung et al. (2016), which refers to clouds at 680 hPa or higher pressure, although we find
182 similar results with or without this restriction.

183 **2.2.1. Meso-scale monthly-mean sampling**

184 This method separates profiles measured in the three campaigns into two groups: those
185 concurrent with a presence of low-level clouds as reported by the HSRL-2 and those concurrent
186 with an absence of any cloud detected by HSRL-2 in the column. The groups are each aggregated
187 into grid boxes approximately 2° by 2° , as shown in Fig. 2. This grid is adapted from Shinozuka et
188 al. (2019) but with additional boxes for the São Tomé-based 2017 and 2018 campaigns. In total,
189 109 hours and 39 hours of flight segments are selected for the cloudy and clear groups,
190 respectively, including minor double-counting where boxes overlap.

191 The arithmetic mean of the CTH of the cloudy group is calculated for each day for each
192 box and 50 m above it is set as the lowest altitude for computing AOD_{ct} for each 10 s period (Sect.
193 2.1). Then the arithmetic mean and standard deviation are calculated for the AOD_{ct} , as well as
194 other measurements (Sect. 2.1, Table 1), for each group and each box. ~~After excluding~~ We exclude
195 the boxes with fewer than 10 counts of 10-second averages and the time periods with mid- and
196 high-level clouds and instrument/aircraft issues, ~~49.~~ Forty-nine hours and ~~26~~ twenty-six hours of
197 the AOD_{ct} measurements enter the analysis for cloudy and clear-sky groups, respectively.

2.2.2. Local-scale near-synchronous sampling

This method identifies cloud edges and demarcates the cloudy side and clear side of each edge based on the time series of the CTH detected by HSRL-2, for level flight legs only. Cloud edges are defined by the points in time when a cloud is detected in a profile adjacent to a profile with no cloud detection.

A clear sky and a cloud are represented by the time period of a certain length, ~~say 60 s~~ in the example illustrated in Fig. 3a, preceding each edge and the same length following it. To ensure that clear skies and clouds are not interrupted for the length, we exclude edges for which another one is found within the length. The longer the length, the smaller the number of cloudy-clear pairs, because longer continuous clouds and clear skies are rarer. Furthermore, we set another length, ~~20 s in the example illustrated in Fig. 3a~~ say 20 s, to exclude immediately before and after the edge, in order to reduce ambiguity associated with a gradual transition from cloud droplets to unactivated particles, the so-called twilight zone (Koren et al., 2007; Schwarz et al., 2017; Várnai and Marshak, 2018). We convert the temporal dimensions into horizontal ones using the mean true horizontal aircraft speed, 200 ms^{-1} for the ER2 (Fig. 3a) and 140 ms^{-1} for the P3 (Fig. 3b and Fig. 3c).

~~We change both the~~ While Fig. 3a has one set of maximum and minimum limits of separation; noted as an example, we alter them in order to assess scale dependence and sampling error as much as our airborne data permit. The way the edges are identified ensures that a measurement cannot be counted more than twice for a given range of separation. A measurement can, however, enter multiple ranges of separation. For example, a measurement 4-6 km away from a cloud edge enters the ranges of 0-6 km, 2-6 km, 2-12 km, 4-12 km, 4-~~24~~20 km, etc. In total, 5.0 hours of horizontal flight are selected, including the double-counting for a given range but excluding the multiple-counting over multiple ranges. Exactly half of them are over clouds. Note that these expressions of separation are only notional; we discuss this in Sect. 4.

As with the meso-scale monthly-mean sampling, we take the arithmetic mean of the CTH of the cloudy side and add 50 m (red lines in Fig. 3). The height is extended to the adjacent clear sky (orange lines) for the calculation of AOD_{ct} (Sect. 2.1). The in situ measurements (Sect. 2.1, Table 1) are each averaged over the cloudy sides and over the clear sides. Cases where aerosol measurements are unavailable for 33% or more of the time period, for example due to calibration or operation problems, are excluded. This makes the number of cloudy-clear pairs vary from

229 property to property for a given range of separation. In total, 3.8 hours of AOD_{ct} measurements
230 enter the analysis.

231 **2.3. Statistical hypothesis testing**

232 We employ the paired t-test, also called paired-samples t-test or dependent t-test, to
233 determine whether the mean difference in each property, Δx (e.g., AOD_{ct}), between the presence
234 and absence of low-level clouds is statistically consistent with the null hypothesis of zero
235 difference. The procedure entails calculating the t statistic, the ratio of the mean cloudy-clear
236 differences to their standard error, E .

$$237 \quad t = \Delta x / E$$

$$238 \quad E = \sigma / \sqrt{N}$$

239 Here the standard error is the standard deviation computed for $N-1$ degrees of freedom, σ , divided
240 by the square root of N , where N is the number of sample pairs. Note that the standard deviation is
241 close to the root-mean-square deviation (RMSD) for small absolute mean difference, unless N is
242 smaller than five.

243 For the calculated t statistic, the two-tailed p value is looked up. Small p values are
244 associated with large t statistics and hence generally large mean differences relative to RMSD. If
245 the p value is smaller than 0.05, we reject the null hypothesis. If it is greater, we do not.

246 The procedure makes several assumptions. One is independence of the differences.
247 Synoptic- and meso-scale phenomena prevalent throughout ORACLES (e.g., subsidence and
248 anticyclones) reduce the independence of the samples. The low day-to-day meteorological
249 variability and repeated flight paths might mean that the same aerosol-cloud conditions were
250 sampled day after day. It is unclear whether this would reduce the independence of the cloudy-
251 clear differences - a potential, seemingly untestable caveat for the meso-scale monthly-mean
252 sampling (Sect. 2.2.1). In the local scale the exclusion of contiguous cloud edges (Sect. 2.2.2)
253 should attain a high level of independence from one another. The procedure also assumes
254 continuous (not discrete), approximately normally distributed data free of outliers.

255 **3. Results**

256 The meso-scale monthly-mean method finds little systematic difference in 532 nm AOD_{ct}
257 (Fig. 4). Most markers lie near the 1:1 line. The mean difference, an indicator of systematic

258 differences, is +0.0201. This is only +169% of the RMSD, an indicator of the total (random and
259 systematic) variability. The p value from the paired t-test is 0.2354. Thus, the AOD above low-
260 level clouds is not significantly different from that at the same heights above nearby clear skies in
261 this scale. The p value is also greater than 0.05 for \log_{10} of AOD_{ct} , something we tested just to
262 confirm that our conclusions do not depend on the choice of linear or log scale. The same goes for
263 the Angstrom exponent and in situ aerosol properties (Table 2, see the rows labeled “box means”).
264 The only exception is the organic mass with a p value just under 0.05 (before rounding).

265 ~~The only exception is the particle number concentration. Four of the 32 horizontal boxes~~
266 ~~see 3-7 times as large concentration over clouds as that over neighboring clear skies (4600-5700~~
267 ~~cm^{-3} vs. 700-2100 cm^{-3}). The mean cloudy-clear difference among all box means is about +40%~~
268 ~~of the RMSD. The t-test yields a p-value of 0.01. One of the assumptions underlying the test, the~~
269 ~~absence of outliers, may be broken in this case.~~

270 The local-scale near-synchronous method finds virtually the same results. The AOD_{ct} is
271 compared in Fig. 5a for 2-6 km separation. The time period corresponds to approximately 10-30 s
272 temporal range on the ER2 (13 data points from the 2016 campaign) and 14-43 s at the average P3
273 speed (53 from 2017 and 2018). All data points lie near the 1:1 line. The mean difference, -0.002,
274 is only -21% of the RMSD for 2-6 km separation. The p value is 0.08.

275 We run the same calculation for other combinations of minimum and maximum separation.
276 Fig. 6 shows the resulting statistics. The mean difference for 2-6 km separation, for example, is
277 represented in Fig. 6a at maximum separation (x axis) of 6 km by the solid orange line that starts
278 after the minimum separation of 2 km. This line also shows that the mean difference is -0.01 if the
279 maximum separation is set to 20 km while keeping the minimum at 2 km. The longest blue line
280 represents the calculations for zero minimum separation (i.e., with the twilight zone included). All
281 other solid lines represent the results with greater minimum separation. For example, the green
282 line that is missing data up to 4 km indicates that the mean difference is closer to -0.01 at 12 km,
283 as shown in Fig. 5b.

284 For the separation up to 20 km, the mean difference is mostly between 0 and -0.01. The p
285 value, shown in Fig. 6b, is below 0.05 for only a handful of the ranges of separation, many most of
286 which, with minimum separation of 0-2 km. ~~This, are subject to potential ambiguity associated~~
287 ~~with the so-called twilight zone (Sect. 2.2.2). Given that a p-value of 0.05 simply means that there~~
288 ~~is a one in 20 chance that the null hypothesis is correct, we expect some low p-values just by~~

289 chance as we conduct many comparisons. The scarcity of low p values is also ~~tr~~evident for log₁₀
290 of AOD_{ct}, the Angstrom exponent and in situ aerosol properties including the ~~number~~
291 ~~concentration~~organic mass (Table 2). Large p values are also found for the ER2- and P3-borne
292 measurements separately and for the 4STAR and the HSRL-2 AOD separately for 2017 and 2018.

293 4. Discussion and ~~Conclusions~~conclusions

294 Virtually no systematic differences in aerosol properties are found between the air above
295 low-level clouds and that above nearby clear areas ~~nearby~~ in ORACLES daytime airborne
296 measurements. The finding holds for a range (0-20 km) of distances between, and expanses of, the
297 two air masses. Note that the temporal and horizontal dimensions associated with the local-scale
298 near-synchronous sampling must be collectively overestimated, because the aircraft may have
299 been running parallel to cloud edge. There is no easy way to know how far from the nearest cloud
300 edge the airplane was in reality. Images from cameras on the plane and satellites may give some
301 context. But we stop short of examining them, ~~discouraged by~~due to the perceived difficulty in
302 unifying the definition of cloud edges between the cameras and the lidar, among other image
303 processing issues. Although we do not know what the real distances and expanses are, that
304 probably does not matter for the region and season of our study, judging by the consistently large
305 p values across the notional distances and expanses. The meso-scale monthly-average sampling,
306 resting on larger data, provides consistent results. ~~Note~~We note that this conclusion may or may
307 not apply to ~~environment~~environments elsewhere, especially those with less uniform clouds.

308 Our analysis does not support aerosol-cloud interactions, circulation patterns or anything
309 else as a cause for a significant systematic difference in aerosol amounts, simply because such a
310 difference is not evident. The lack of obvious sensitivity to the smoke-cloud gap height, indicated
311 by marker color in Fig. 5, is consistent with this conclusion. The smoke bottom height minus the
312 mean CTH gives an estimate of whether aerosols may be physically in contact with clouds and
313 therefore there is a chance of wet removal- and cloud processing. Our analysis does not detect any
314 sign of local aerosol removal by the underlying clouds.

315 An important difference between the present analysis and the CALIOP-based one (~~Chung~~
316 ~~et al., 2016~~);(Chung et al., 2016), apart from the spatiotemporal range and resolution, is that the
317 HSRL algorithm (~~Hair et al., 2008~~) does not use any explicit layer detection- (Hair et al., 2008).
318 The return signal in the molecular signal provides a measure of the aerosol attenuation and

319 extinction. A very tenuous aerosol layer still produces a reported extinction with a reported error
320 bar. If the aerosol extinction is very small, the error bar may exceed the retrieved value, but there
321 is no cutoff at small values that produces the kind of bias one gets from a detection threshold.
322 Furthermore, the ~~signal-to-noise~~S/N ratio is higher than that of CALIOP and no assumptions about
323 lidar ratio are made, as explained in Sect. 2.1.

324 We posit that the systematic differences between above-cloud and clear skies AODs shown
325 in Chung et al. ~~(2016)~~(2016) are *solely* a CALIOP retrieval artifact, at least for the ORACLES
326 region and season. As ~~the authors discuss~~described in Sect. 1, the CALIOP standard algorithm has
327 a detection bias. ~~The algorithm confines itself that leads to distinct aerosol layers whose~~
328 ~~signals~~greater AOD underestimates over clouds than in clear skies by day due to upward sunlight
329 reflection. The authors emphasize that this bias might explain their results, pointing to a day-night
330 contrast as evidence: “a corresponding difference cannot be seen in the ΔAOD_{ct} derived from
331 nighttime retrievals [which are high enough compared to detector noise and, during free of sunlight
332 reflection]”. The present study corroborates this hypothesis, by rejecting the day, solar background
333 light. If other possible explanations related to aerosol amounts.

334 We should note that the signal-to-noise detection bias due to a low S/N ratio of a layer is
335 not high enough, no extinction is reported for the portion only known source of error in the daytime
336 CALIOP standard AOD product. The error can also originate from a misclassified aerosol profile;
337 summing up type and, hence, an incorrectly assumed lidar ratio in the extinction produces a low-
338 biased AOD. CALIOP algorithm. Such an aerosol misclassification can either over- or under-
339 estimate CALIOP AOD, unlike an undetected aerosol layer. Misclassification and low S/N ratio,
340 taken together, explain the absence of a significant bias between CALIOP and HSRL-1 above-
341 cloud AODs in a low aerosol-above-cloud environment such as over Northern America in
342 Kacenelenbogen et al. (2014). On the other hand, Liu et al. (2015) describe a CALIOP standard
343 daytime AOD underestimate above clouds over two regions of high above-cloud AODs. While
344 both misclassification and low S/N ratio are at play, Liu et al. (2015) mainly explain the CALIOP
345 above-cloud AOD underestimate by a low S/N ratio (especially when solar light is reflected on the
346 underlying cloud) in the case of smoke in South East Atlantic, and an underestimate of the lidar
347 ratio in the case of Saharan dust (see their Table 2).

348 The depolarization/multiple scattering method by Hu et al. In Chung et al. (2016), the lower
349 daytime CALIOP AOD above clouds can be explained mainly by CALIOP’s low S/N ratio as

350 there is no reason to believe that CALIOP would show a different classification bias above clouds
351 compared to nearby clear skies. The depolarization ratio method by Hu et al. (2007) retrieves
352 above-cloud AOD from CALIOP without a layer detection algorithm. This method may lead to a
353 different result from Chung et al. (2016). A future study based on the Hu et al. (2007) method and
354 extended to the globe as in Kacenelenbogen et al. (2019) will also address
355 ~~environment~~environments under a wider variety of synoptic- and meso-scale conditions that
356 produce specific opaque water clouds.

357 The Going back to the present aircraft-based study, the absence of systematic differences is
358 good news, because satellite retrievals and studies of radiative effects do not need to treat these
359 two conditions as different. Our results on AOD_{ct} justify, for example, temporal and horizontal
360 extrapolation of above-cloud AOD to adjacent clear skies and attribution of the difference from
361 full-column AOD to the planetary boundary layer. Our results on the aerosol intensive properties
362 suggest that a single set of aerosol models can be used for the aerosols in the free troposphere
363 regardless of whether clouds exist below, which may allow better characterization of the
364 underlying clouds and the radiative effects (Matus et al., 2015; Meyer et al., 2015). It seems
365 reasonable to use aerosol properties retrieved in clear skies for estimating the direct radiative
366 effects of aerosols above nearby clouds, as in Kacenelenbogen et al. (2019). But challenges
367 remain. Random variability in AOD and other aerosol properties is significant, as indicated by
368 RMSD in the present study and quantified for smoke elsewhere (Shinozuka and Redemann, 2011).
369 It may be problematic to assume the same values for intensive properties for reasons not
370 investigated here, for example: form of combustion, degree of aerosol ageing and influence of the
371 boundary layer. These may be tackled more effectively by combining sensors of various
372 capabilities with improved spatiotemporal resolution and retrieval algorithms (~~National~~
373 ~~Academies of Sciences, Engineering, and Medicine et al., 2019~~). Improved
374 spatiotemporal(National Academies of Sciences, Engineering, and Medicine, 2018). These
375 improved satellite observations of aerosol properties in clear skies and above clouds are urgently
376 needed to reduce the uncertainty in total aerosol radiative forcing (~~National Academies of~~
377 ~~Sciences, Engineering, and Medicine et al., 2019~~). For this, we are looking forward to the next
378 generation of space-borne lidars, radars, microwave radiometers, polarimeters and spectrometers
379 such as the ones that will address joint Aerosols, Clouds, Convection and Precipitation (ACCP)
380 science goals and objectives (<https://science.nasa.gov/earth-science/decadal-accp>)

381 **Data availability**

382 The P3 and ER2 observational data (~~ORACLES Science Team, 2017, 2019~~) are available
383 ~~through www.espo.nasa.gov/oracles~~ (~~ORACLES Science Team, 2020a, 2020b~~) are available
384 ~~through http://dx.doi.org/10.5067/Suborbital/ORACLES/P3/2016_V2~~ and
385 ~~http://dx.doi.org/10.5067/Suborbital/ORACLES/ER2/2016_V2~~.

386 **Author contribution**

387 All authors participated in the investigation during the ORACLES intensive observation
388 periods. In addition, MSK led conceptualization, funding acquisition, methodology, project
389 administration and supervision. YS led data curation, formal analysis, software and validation and
390 wrote the original draft. YS and MSK contributed visualization. All but CJF reviewed and edited
391 the manuscript.

392 **Competing interests**

393 The authors declare that they have no conflict of interest.

394 **Acknowledgments**

395 ~~We thank Eric Wileox,~~ We would like to thank Eric Wilcox and one anonymous referee for
396 reading the manuscript and providing valuable comments. In addition, we thank Tamás Várnai and
397 Sasha Marshak for discussion. ORACLES is funded by NASA Earth Venture Suborbital-2 grant
398 NNH13ZDA001N-EVS2.

399 **References**

- 400 Anderson, T. L. and Ogren, J. A.: Determining aerosol radiative properties using the TSI 3563 integrating
401 nephelometer, *Aerosol Sci. Technol.*, 29, 57–69, 1998.
- 402 Burton, S. P., Ferrare, R. A., Hostetler, C. A., Hair, J. W., Rogers, R. R., Obland, M. D., Butler, C. F.,
403 Cook, A. L., Harper, D. B. and Froyd, K. D.: Aerosol classification using airborne High Spectral
404 Resolution Lidar measurements – methodology and examples, *Atmospheric Measurement Techniques*,
405 5(1), 73–98, 2012.
- 406 Burton, S. P., Hostetler, C. A., Cook, A. L., Hair, J. W., Seaman, S. T., Scola, S., Harper, D. B., Smith, J.
407 A., Fenn, M. A., Ferrare, R. A., Saide, P. E., Chemyakin, E. V. and Müller, D.: Calibration of a high

408 spectral resolution lidar using a Michelson interferometer, with data examples from ORACLES, Appl.
409 Opt., 57(21), 6061–6075, 2018.

410 Chung, C. E., Lewinschal, A. and Wilcox, E.: Relationship between low-cloud presence and the amount
411 of overlying aerosols, Atmos. Chem. Phys., 16(9), 5781–5792, 2016.

412 Costantino, L. and Bréon, F.-M.: Analysis of aerosol-cloud interaction from multi-sensor satellite
413 observations, Geophys. Res. Lett., 37(11), doi:10.1029/2009gl041828, 2010.

414 Costantino, L. and Bréon, F.-M.: Aerosol indirect effect on warm clouds over South-East Atlantic, from
415 co-located MODIS and CALIPSO observations, Atmos. Chem. Phys., 13(1), 69–88, 2013.

416 DeCarlo, P. F., Kimmel, J. R., Trimborn, A., Northway, M. J., Jayne, J. T., Aiken, A. C., Gonin, M.,
417 Fuhrer, K., Horvath, T., Docherty, K. S., Worsnop, D. R. and Jimenez, J. L.: Field-Deployable, High-
418 Resolution, Time-of-Flight Aerosol Mass Spectrometer, Anal. Chem., 78(24), 8281–8289, 2006.

419 ~~Diamond, M. S., Dobracki, A., Freitag, S., Small-Griswold, J. D., Heikkila, A., Howell, S. G., Kacarab,~~
420 ~~M. E., Podolske, J. R., Saide, P. E. and Wood, R.: Time dependent entrainment of smoke presents an~~
421 ~~observational challenge for assessing aerosol–cloud interactions over the southeast Atlantic Ocean,~~
422 ~~Atmos. Chem. Phys., 18(19), 14623–14636, 2018.~~

423 Dunagan, S. E., Johnson, R., Zavaleta, J., Russell, P. B., Schmid, B., Flynn, C., Redemann, J., Shinozuka,
424 Y., Livingston, J. and Segal-Rosenhaimer, M.: Spectrometer for Sky-Scanning Sun-Tracking
425 Atmospheric Research (4STAR): Instrument Technology, Remote Sensing, 5(8), 3872–3895, 2013.

426 Hair, J. W., Hostetler, C. A., Cook, A. L., Harper, D. B., Ferrare, R. A., Mack, T. L., Welch, W.,
427 Izquierdo, L. R. and Hovis, F. E.: Airborne High Spectral Resolution Lidar for profiling aerosol optical
428 properties, Appl. Opt., 47(36), 6734–6752, 2008.

429 Hu, Y., Vaughan, M., Liu, Z., Powell, K. and Rodier, S.: Retrieving Optical Depths and Lidar Ratios for
430 Transparent Layers Above Opaque Water Clouds From CALIPSO Lidar Measurements, IEEE
431 Geoscience and Remote Sensing Letters, 4(4), 523–526, 2007.

432 Johnson, B. T., Shine, K. P. and Forster, P. M.: The semi-direct aerosol effect: Impact of absorbing
433 aerosols on marine stratocumulus, Quarterly Journal of the Royal Meteorological Society, 130(599),
434 1407–1422, doi:10.1256/qj.03.61, 2004.

435 Kacenelenbogen, M., Redemann, J., Vaughan, M. A., Omar, A. H., Russell, P. B., Burton, S., Rogers, R.
436 R., Ferrare, R. A. and Hostetler, C. A.: An evaluation of CALIOP/CALIPSO’s aerosol-above-cloud
437 detection and retrieval capability over North America, J. Geophys. Res. D: Atmos., 119(1), 230–244,
438 2014.

439 Kacenelenbogen, M. S., Vaughan, M. A., Redemann, J., Young, S. A., Liu, Z., Hu, Y., Omar, A. H.,
440 LeBlanc, S., Shinozuka, Y., Livingston, J. and Others: Estimations of global shortwave direct aerosol
441 radiative effects above opaque water clouds using a combination of A-Train satellite sensors, Atmos.
442 Chem. Phys., 19(7), 4933–4962, 2019.

443 Koren, I., Remer, L. A., Kaufman, Y. J., Rudich, Y. and Vanderlei Martins, J.: On the twilight zone
444 between clouds and aerosols, Geophysical Research Letters, 34(8), doi:10.1029/2007g1029253, 2007.

445 LeBlanc, S. E., Redemann, J., Flynn, C., Pistone, K., Kacenelenbogen, M., Segal-Rosenheimer, M.,
446 Shinozuka, Y., Dunagan, S., Dahlgren, R. P., Meyer, K., Podolske, J., Howell, S. G., Freitag, S., Small-

- 447 Griswold, J., Holben, B., Diamond, M., Formenti, P., Piketh, S., Maggs-Kölling, G., Gerber, M. and
448 Namwoonde, A.: Above Cloud Aerosol Optical Depth from airborne observations in the South-East
449 Atlantic, , doi:10.5194/acp-2019-43, 2019.
- ~~450 Liu, Z., Winker, D., Omar, A., Vaughan, M., Kar, J., Trepte, C., Hu, Y. and Schuster, G.: Evaluation of
451 CALIOP 532-nm aerosol optical depth over opaque water clouds, Atmos. Chem. Phys., 15(3), 1265–
452 1288, 2015.~~
- 453 Matus, A. V., L’Ecuyer, T. S., Kay, J. E., Hannay, C. and Lamarque, J.-F.: The Role of Clouds in
454 Modulating Global Aerosol Direct Radiative Effects in Spaceborne Active Observations and the
455 Community Earth System Model, J. Clim., 28(8), 2986–3003, 2015.
- 456 Meyer, K., Platnick, S. and Zhang, Z.: Simultaneously inferring above-cloud absorbing aerosol optical
457 thickness and underlying liquid phase cloud optical and microphysical properties using MODIS, J.
458 Geophys. Res. D: Atmos., 120(11), 5524–5547, 2015.
- ~~459 National Academies of Sciences, Engineering, and Medicine, Division on Engineering and Physical
460 Sciences, Space Studies Board and Committee on the Decadal Survey for Earth Science and Applications
461 from Space: Thriving on Our Changing Planet: A Decadal Strategy for Earth Observation from Space,
462 National Academies Press., 2019.~~
- ~~463 ORACLES Science Team: Suite of Aerosol, Cloud, and Related Data Acquired Aboard ER2 During
464 ORACLES 2016, Version 1, , doi:10.5067/SUBORBITAL/ORACLES/ER2/2016_V1, 2017.~~
- ~~465 ORACLES Science Team: Suite of Aerosol, Cloud and Related Data Acquired Aboard P3 During
466 ORACLES 2017, Version 1, , doi:10.5067/SUBORBITAL/ORACLES/P3/2017_V1, 2019.~~
- ~~467 National Academies of Sciences, Engineering, and Medicine: Thriving on Our Changing Planet: A
468 Decadal Strategy for Earth Observation from Space, The National Academies Press, Washington, DC.,
469 2018.~~
- ~~470 ORACLES Science Team: Suite of Aerosol, Cloud, and Related Data Acquired Aboard ER2 During
471 ORACLES 2016, Version 2, , doi:10.5067/Suborbital/ORACLES/ER2/2016_V2, 2020a.~~
- ~~472 ORACLES Science Team: Suite of Aerosol, Cloud, and Related Data Acquired Aboard P3 During
473 ORACLES 2016, Version 2, , doi:10.5067/Suborbital/ORACLES/P3/2016_V2, 2020b.~~
- 474 Pistone, K., Redemann, J., Doherty, S., Zuidema, P., Burton, S., Cairns, B., Cochrane, S., Ferrare, R.,
475 Flynn, C., Freitag, S., Howell, S. G., Kacenelenbogen, M., LeBlanc, S., Liu, X., Schmidt, K. S., Sedlacek,
476 A. J., III, Segal-Rozenhaimer, M., Shinozuka, Y., Stammes, S., van Diedenhoven, B., Van Harten, G. and
477 Xu, F.: Intercomparison of biomass burning aerosol optical properties from in situ and remote-sensing
478 instruments in ORACLES-2016, Atmos. Chem. Phys., 19(14), 9181–9208, 2019.
- 479 Redemann, Wood, Zuidema, Doherty, Luna, LeBlanc, Diamond, Shinozuka, Ueyama, Pfister, DaSilva,
480 Longo, Kacenelenbogen, Knox, Piketh, Haywood, Formenti, Mallet, Stier, Ackerman, Carmichael, Saide,
481 Howell, Cairns, Knobelspiesse, Tanelli, L’Ecuyer, McFarquhar, Poellot, Nenes, Kacarab, Pui Shan
482 Wong, Small-Griswold, Thornhill, Noone, Podolske, Schmidt, Sedlacek, Lang, Stith, Segal-Rozenhaimer,
483 Hostetler, Ferrare, Burton, Diner, Platnick, Myers, Meyer, Spangenberg, Ian Chang: An overview of the
484 ORACLES (ObSERVations of Aerosols above CLouds and their intERactionS) project: aerosol-cloud-
485 radiation interactions in the Southeast Atlantic basin, n.d. in preparation.

486

487 Rogers, R. R., Hair, J. W., Hostetler, C. A., Ferrare, R. A., Obland, M. D., Cook, A. L., Harper, D. B.,
488 Burton, S. P., Shinozuka, Y., McNaughton, C. S., Clarke, A. D., Redemann, J., Russell, P. B., Livingston,
489 J. M. and Kleinman, L. I.: NASA LaRC airborne high spectral resolution lidar aerosol measurements
490 during MILAGRO: observations and validation, *Atmos. Chem. Phys.*, 9(14), 4811–4826, 2009.

491 [Sayer, A. M., Hsu, N. C., Lee, J., Kim, W. V., Burton, S., Fenn, M. A., Ferrare, R. A., Kacenelenbogen,](#)
492 [M., LeBlanc, S., Pistone, K., Redemann, J., Segal-Rozenhaimer, M., Shinozuka, Y. and Tsay, S.-C.: Two](#)
493 [Decades Observing Smoke Above Clouds in the South-Eastern Atlantic Ocean: Deep Blue Algorithm](#)
494 [Updates and Validation with ORACLES Field Campaign Data, \[online\] Available from:](#)
495 <https://ntrs.nasa.gov/search.jsp?R=20190028671> (Accessed 5 June 2020), 2019.

496 Schwarz, K., Cermak, J., Fuchs, J. and Andersen, H.: Mapping the Twilight Zone—What We Are
497 Missing between Clouds and Aerosols, *Remote Sensing*, 9(6), 577, 2017.

498 Shinozuka, Y. and Redemann, J.: Horizontal variability of aerosol optical depth observed during the
499 ARCTAS airborne experiment, *Atmos. Chem. Phys.*, 11(16), 8489–8495, 2011.

500 Shinozuka, Y., Johnson, R. R., Flynn, C. J., Russell, P. B., Schmid, B., Redemann, J., Dunagan, S. E.,
501 Kluzek, C. D., Hubbe, J. M., Segal-Rosenheimer, M., Livingston, J. M., Eck, T. F., Wagener, R.,
502 Gregory, L., Chand, D., Berg, L. K., Rogers, R. R., Ferrare, R. A., Hair, J. W., Hostetler, C. A. and
503 Burton, S. P.: Hyperspectral aerosol optical depths from TCAP flights, *J. Geophys. Res. D: Atmos.*,
504 2013JD020596, 2013.

505 Shinozuka, Y., Saide, P. E., Ferrada, G. A., Burton, S. P., Ferrare, R., Doherty, S. J., Gordon, H., Longo,
506 K., Mallet, M., Feng, Y., Wang, Q., Cheng, Y., Dobracki, A., Freitag, S., Howell, S. G., LeBlanc, S.,
507 Flynn, C., Segal-Rosenhaimer, M., Pistone, K., Podolske, J. R., Stith, E. J., Bennett, J. R., Carmichael, G.
508 R., da Silva, A., Govindaraju, R., Leung, R., Zhang, Y., Pfister, L., Ryoo, J.-M., Redemann, J., Wood, R.
509 and Zuidema, P.: Modeling the smoky troposphere of the southeast Atlantic: a comparison to ORACLES
510 airborne observations from September of 2016, *Aerosols/Field Measurements/Troposphere/Chemistry*
511 (chemical composition and reactions), doi:10.5194/acp-2019-678, 2019.

512 Shipley, S. T., Tracy, D. H., Eloranta, E. W., Trauger, J. T., Sroga, J. T., Roesler, F. L. and Weinman, J.
513 A.: High spectral resolution lidar to measure optical scattering properties of atmospheric aerosols. 1:
514 Theory and instrumentation, *Appl. Opt.*, AO, 22(23), 3716–3724, 1983.

515 Stier, P., Schutgens, N. A. J., Bellouin, N., Bian, H., Boucher, O., Chin, M., Ghan, S., Huneus, N.,
516 Kinne, S., Lin, G., Ma, X., Myhre, G., Penner, J. E., Randles, C. A., Samset, B., Schulz, M., Takemura,
517 T., Yu, F., Yu, H. and Zhou, C.: Host model uncertainties in aerosol radiative forcing estimates: results
518 from the AeroCom Prescribed intercomparison study, *Atmos. Chem. Phys.*, 13(6), 3245–3270, 2013.

519 Várnai, T. and Marshak, A.: Satellite Observations of Cloud-Related Variations in Aerosol Properties,
520 *Atmosphere*, 9(11), 430, doi:10.3390/atmos9110430, 2018.

521 Virkkula, A.: Correction of the Calibration of the 3-wavelength Particle Soot Absorption Photometer (3λ
522 PSAP), *Aerosol Sci. Technol.*, 44(8), 706–712, 2010.

523 Waquet, F., Peers, F., Ducos, F., Goloub, P., Platnick, S., Riedi, J., Tanré, D. and Thieuleux, F.: Global
524 analysis of aerosol properties above clouds, *Geophys. Res. Lett.*, 40(21), 5809–5814, 2013.

525 Wilcox, E. M.: Stratocumulus cloud thickening beneath layers of absorbing smoke aerosol, *Atmos. Chem.*
526 *Phys.*, 10(23), 11769–11777, 2010.

- 527 Winker, D. M., Vaughan, M. A., Omar, A., Hu, Y., Powell, K. A., Liu, Z., Hunt, W. H. and Young, S. A.:
528 Overview of the CALIPSO Mission and CALIOP Data Processing Algorithms, *J. Atmos. Ocean.*
529 *Technol.*, 26(11), 2310–2323, 2009.
- 530 Zuidema, P., Redemann, J., Haywood, J., Wood, R., Piketh, S., Hipondoka, M. and Formenti, P.: Smoke
531 and clouds above the southeast Atlantic: Upcoming field campaigns probe absorbing aerosol's impact on
532 climate, *Bull. Am. Meteorol. Soc.*, 97(7), 1131–1135, 2016.
- 533

Table 1. Properties and instruments used in this study and the altitudes they refer to.

Property	September 2016 on the ER2 aircraft		August 2017 and October 2018* on the P3 aircraft	
	Instrument	Altitude	Instrument	Altitude
cloud top height (CTH)	HSRL-2	limited Limited to ≤ 3241 m in this study	HSRL-2	no No higher than 500 m below the P3 and ≤ 3241 m
aerosol optical depth above cloud top height (AOD _{ct})	HSRL-2	from ~50 m above the CTH to 14 km	4STAR HSRL-2 and 4STAR	from the P3 to top of atmosphere (TOA), when the P3 is 500-1500 m above CTH from ~50 m above the CTH to TOA, except 0-1500 m below the P3, when the P3 is >1500 m above CTH
extinction coefficient, single scattering albedo, submicron non-refractory organic mass, number concentration	-	-	nephelometer, PSAP, HR-ToF AMS and condensation particle counter	at the P3 when the P3 is 500-1500 m above CTH

535 * One day in September 2017 and two days in September 2018 are also included.

536 - Not presented in this study. Observations were made from the P3, away from the ER2 for most
537 cases.

538

539

540

Table 2. Statistics The mean values and the statistics on the cloudy-clear differences

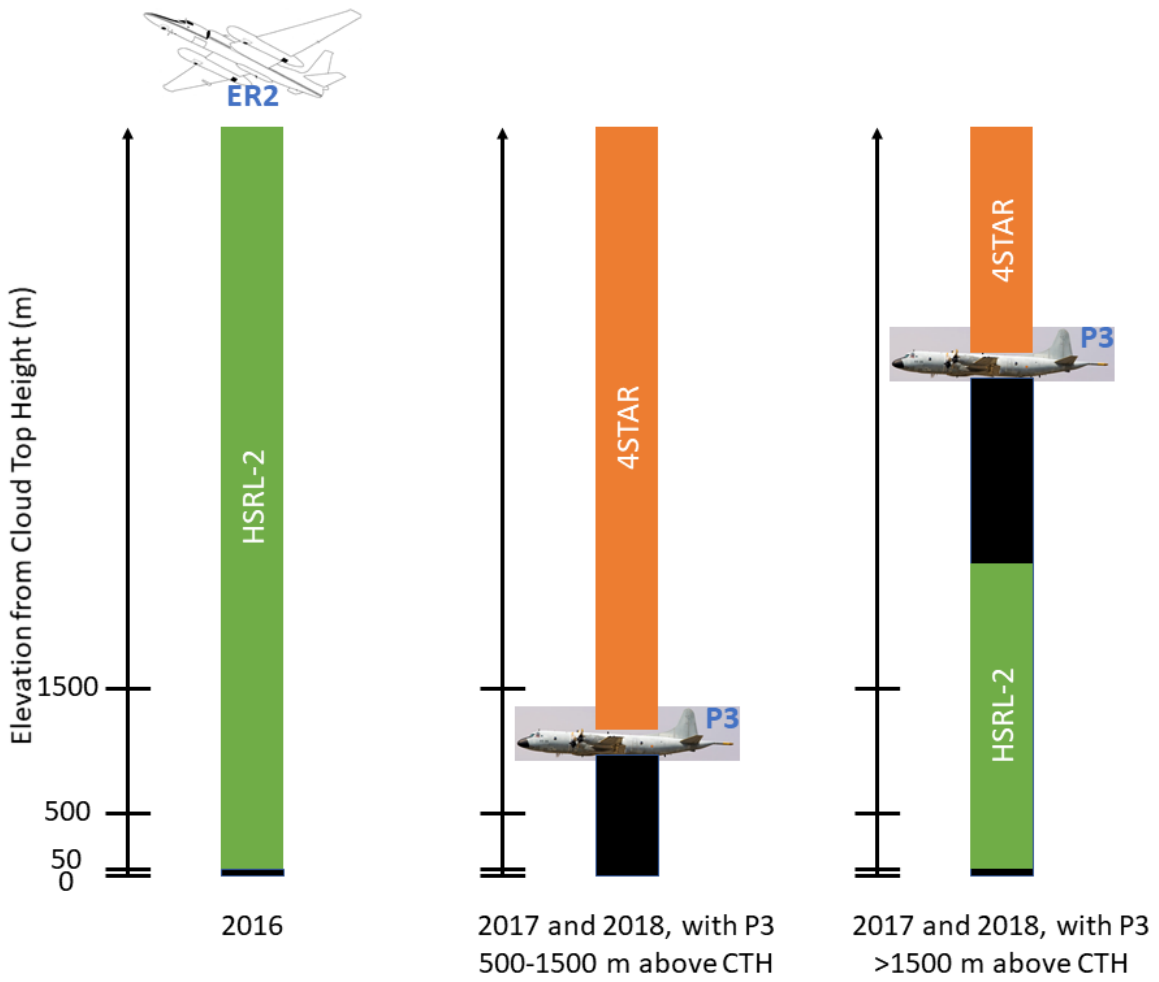
Sampling*	<u>Mean</u>	Mean Difference	RMSD	p	Number of Pairs
532 nm AOD _{ct}					
2-6 km	<u>0.34</u>	-0.00	0.01	0.08	66
4-12 km	<u>0.34</u>	-0.01	0.02	0.23	18
box means	<u>+0.0228</u>	<u>+0.1201</u>	<u>0.2310</u>	<u>0.54</u>	<u>46</u>
log ₁₀ 532 nm AOD _{ct}					
2-6 km	<u>-0.53</u>	-0.00	0.01	0.15	66
4-12 km	<u>-0.53</u>	-0.00	0.02	0.27	18
box means	<u>-0.68</u>	<u>+0.0503</u>	<u>0.1918</u>	<u>0.0721</u>	<u>5446</u>
Angstrom Exponent of AOD _{ct}					
2-6 km	<u>1.19</u>	-0.04	0.11	0.00	53
4-12 km	<u>1.30</u>	-0.02	0.05	0.08	16
box means	<u>1.13</u>	<u>-0.0201</u>	0.10	<u>0.1463</u>	<u>5443</u>
In Situ 550 nm Extinction Coefficient (Mm ⁻¹)					
2-6 km	<u>67.0</u>	-0.2	3.0	0.87	7
4-12 km	<u>84.6</u>	-3.6	5.1	0.31	3
box means	<u>+19.064.1</u>	<u>67.9+14.6</u>	<u>71.8</u>	<u>0.1838</u>	<u>2420</u>
In Situ 550 nm Single Scattering Albedo					
2-6 km	<u>0.85</u>	-0.00	0.01	0.14	7
4-12 km	<u>0.87</u>	-0.01	0.01	0.35	3
box means	<u>-0.0084</u>	<u>+0.01</u>	0.05	<u>0.9957</u>	<u>2420</u>

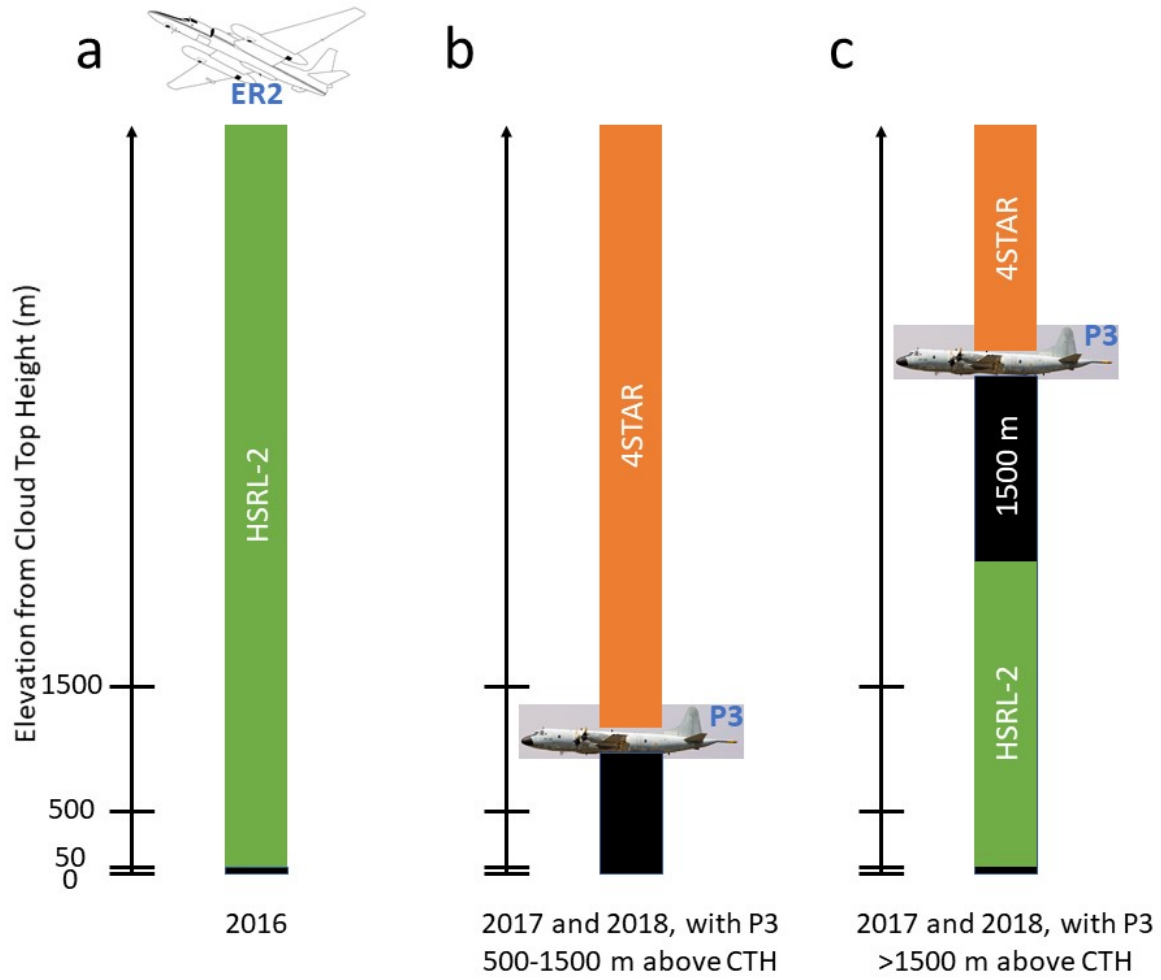
Submicron Non-refractory Aerosol Organic Mass (µg µg m ⁻³)					
2-6 km	<u>6.5</u>	+0.1	0.5	0.75	9
4-12 km	<u>6.1</u>	-0.4	0.6	0.38	3
box means	<u>7.0</u>	+1. <u>29</u>	4. <u>45</u>	0. <u>1405</u>	<u>2822</u>
Number Concentration of Particles >10 nm (cm ⁻³)					
2-6 km	<u>1903</u>	<u>±5</u>	59	0.82	10
4-12 km	<u>2378</u>	-110	121	0.09	3
box means	<u>6141574</u>	<u>1411+239</u>	<u>962</u>	0. <u>0117</u>	<u>3122</u>

542

* Either the ~~temporal~~ separation from cloud edges or box means.

543



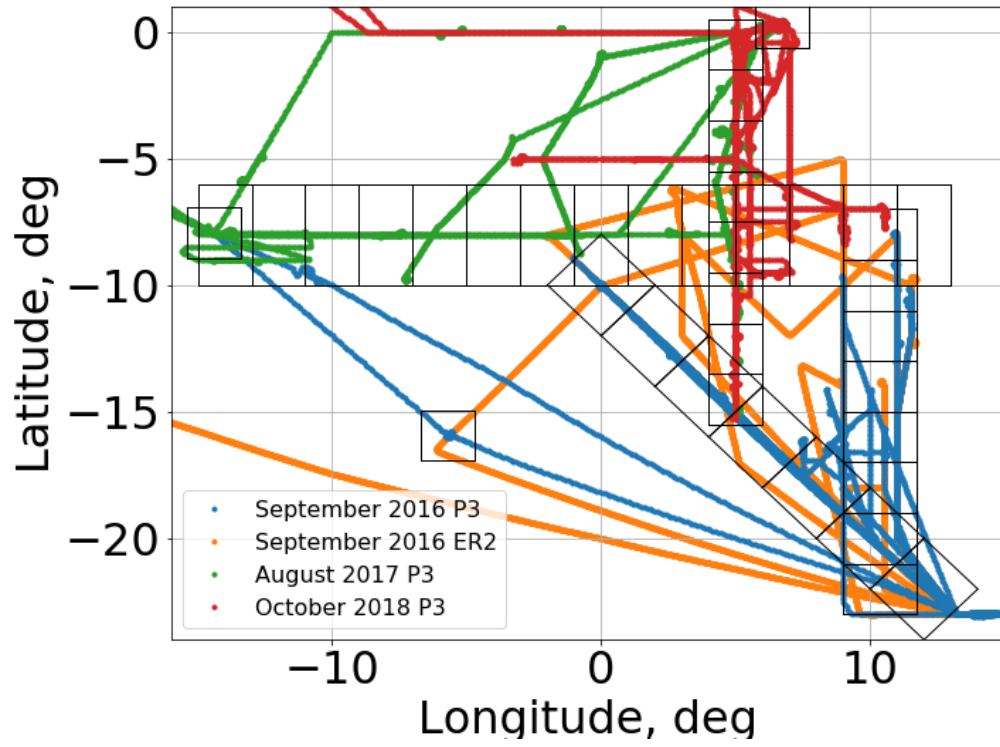


545

546

Figure 1. AOD above cloud top height (AOD_{ct}). See text and Table 1 for details.

547



548

549

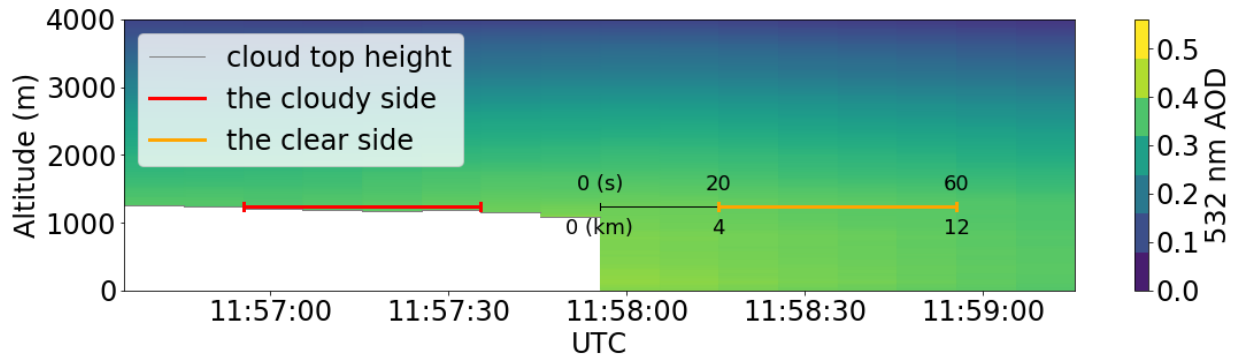
550

Figure 2. The flight paths of ORACLES. The boxes for meso-scale monthly-mean sampling are superimposed.

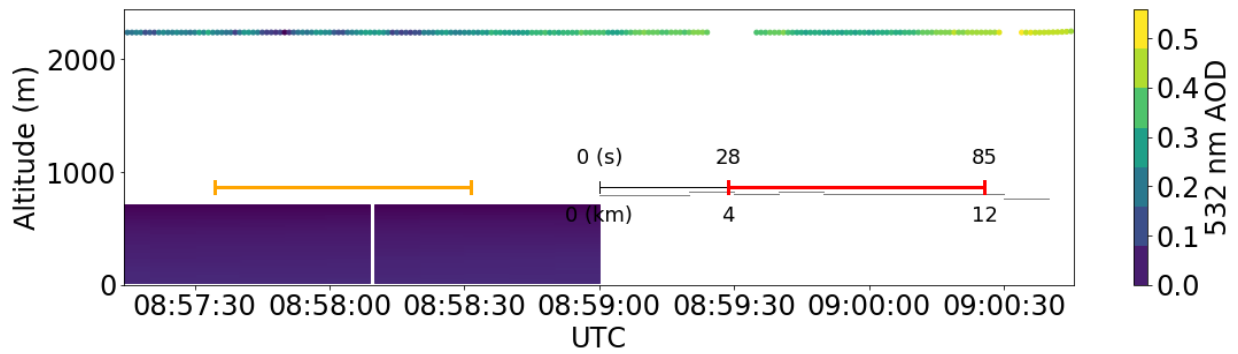
551

552

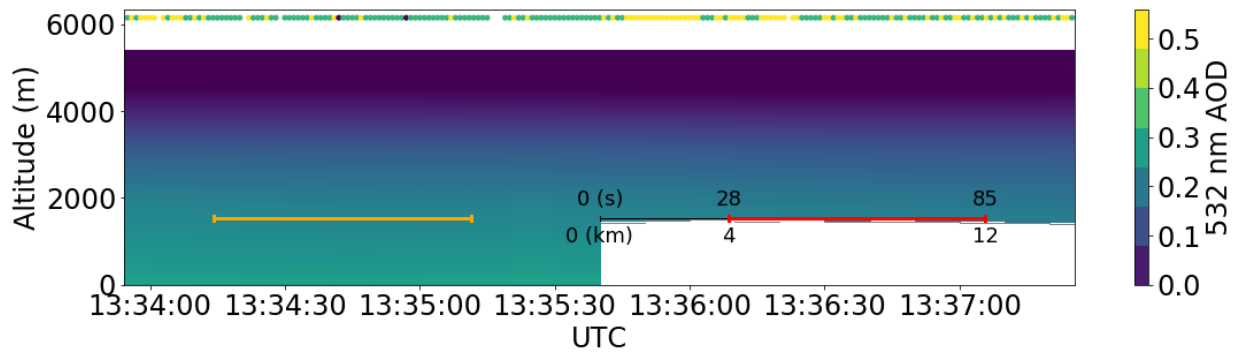
553



554

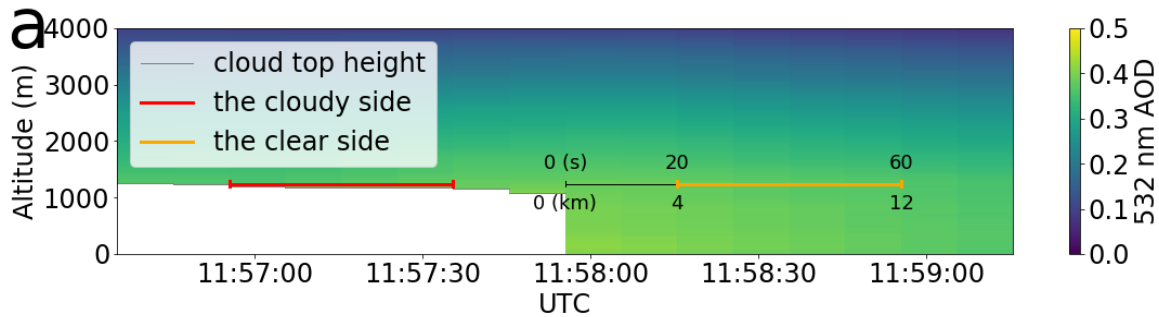


555

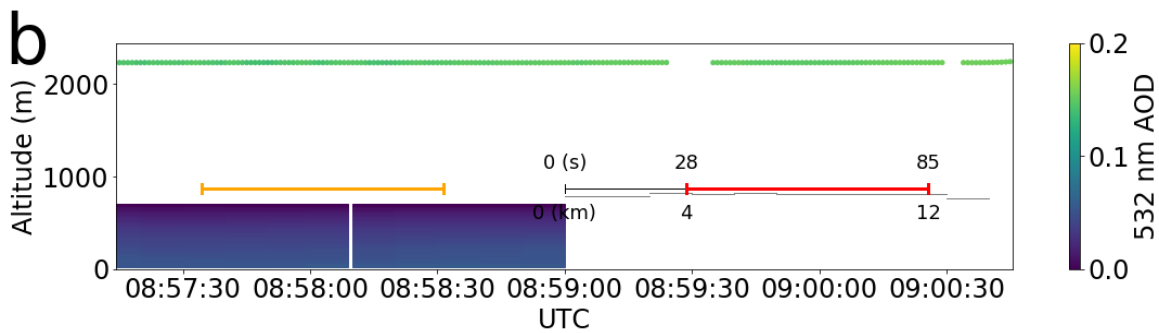


556

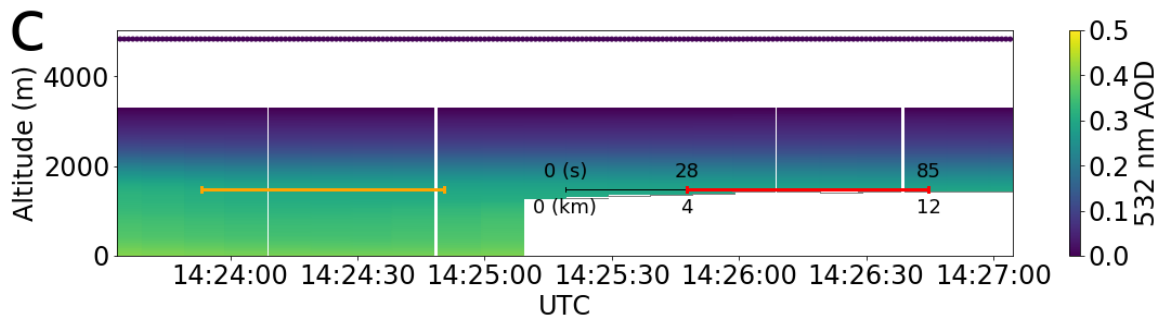
557



558



559



560

561

562

563

564

565

566

567

568

569

570

571

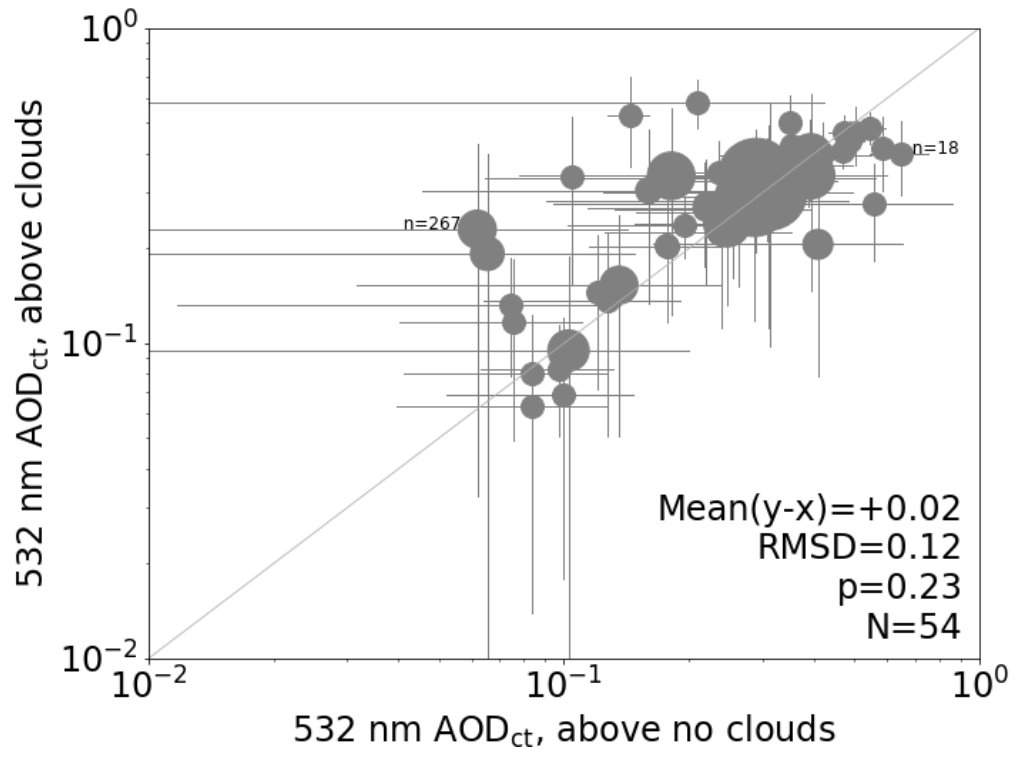
572

Figure 3. (a) Local Examples of local-scale near-synchronous sampling, based on the HSRL-2 cloud top height (CTH) product; (a) In this subset of the ER2 flight on September 12, 2016, a cloud edge is found at 11:57:56, (denoted by 0 s and 0 km). The cloudy and clear side, each with horizontal separation of 4-12 km measured from cloud edge, are marked by red and orange lines, respectively. The HSRL-2 AOD profiles are given for altitudes from ~50 m above the CTH, clouds (as in Fig. 1a). (b) ~~An example of local-scale near-synchronous sampling from the P3 aircraft with both HSRL-2 and 4STAR onboard.~~ With the P3 500-1500 m above the CTH, (Fig. 1b), as is the case with this example from October 5, 2018, we use 4STAR AOD only. The 4STAR AOD is indicated at the P3 altitudes just above 2000 m but refers to all altitudes above them. (c) ~~Another example of local-scale near-synchronous sampling from~~ With the P3 aircraft ~~with both HSRL-2 and 4STAR onboard.~~ For the time periods when it flew >1500 m above the CTH, (Fig. 1c), as is the case for this example from ~~October 15, 2018~~ August 12, 2017, the 4STAR AOD, indicated at the P3 altitudes just above

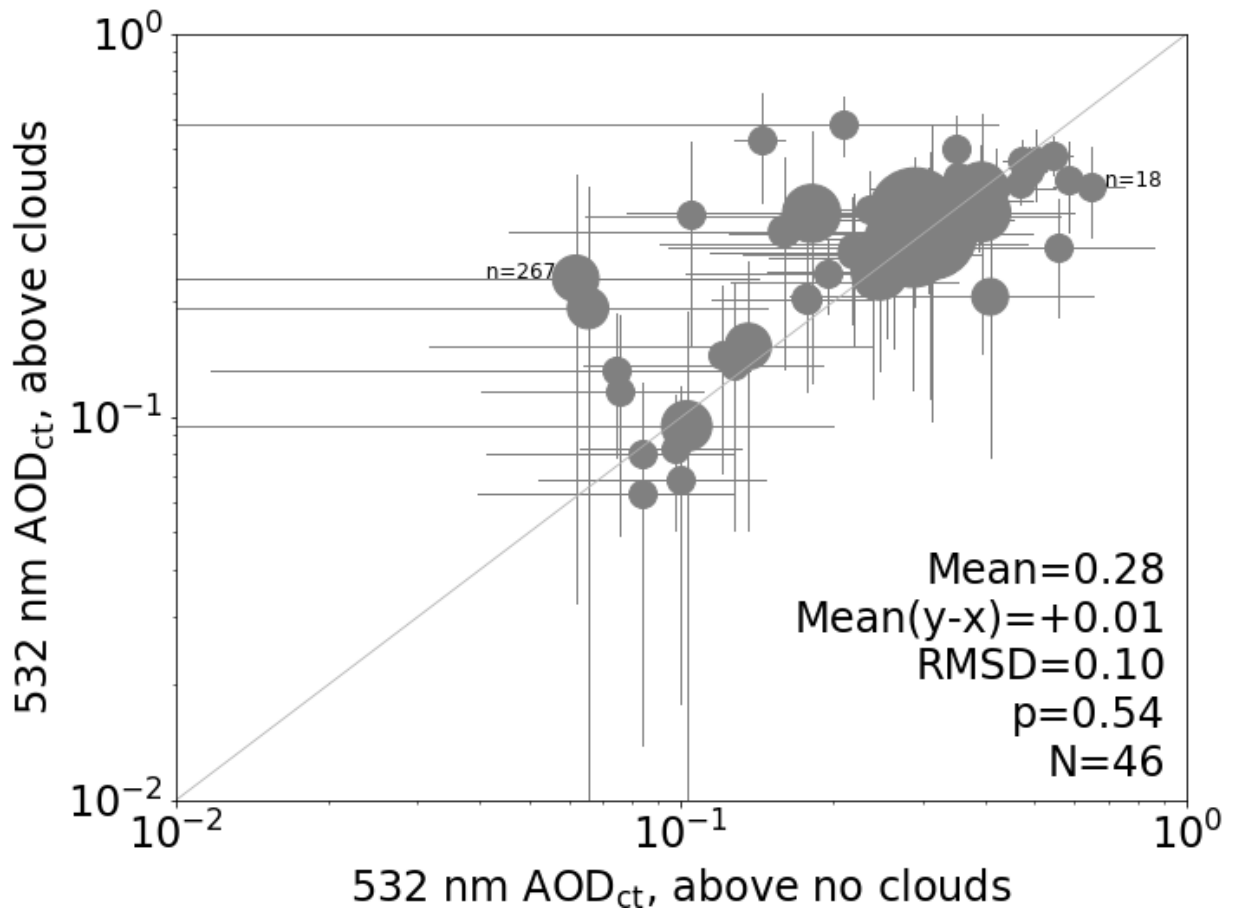
573 ~~6000~~under 5000 m, is added to the HSRL-2 AOD at ~50 m above the CTH. The upper limit
574 of the integral of extinction is 1500 m below the P3 altitude.

575

576



577
578



579

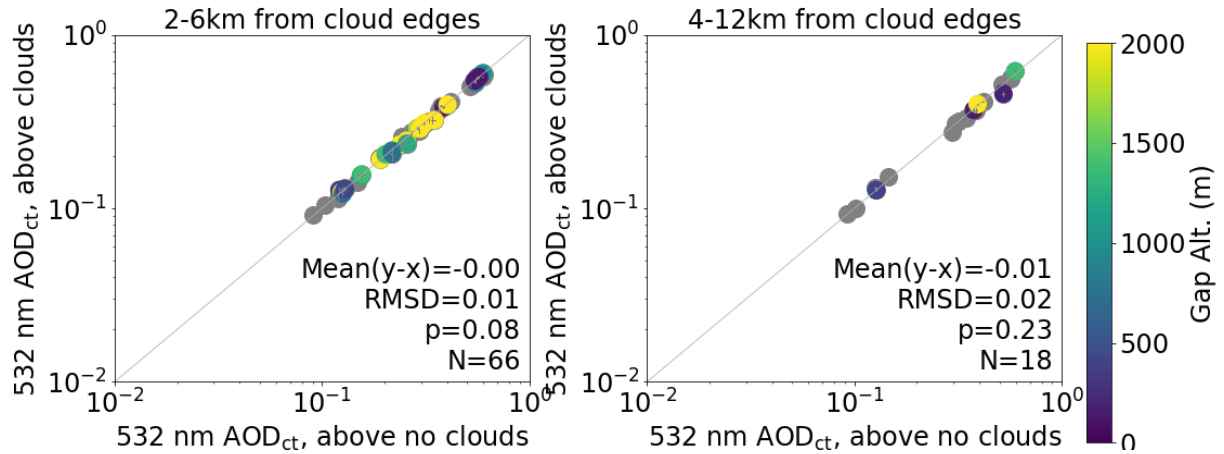
580 **Figure 4. The meso-scale monthly-mean samples of the AOD above cloud top height.**
581 **Each marker represents the mean over a box shown in Fig. 2. The bar represents the**
582 **± 1 standard deviation range. The marker size is proportional to the number (n) of**
583 **s measurements for each combination of box and month, the fewer of the cloudy and**
584 **clear groups. N refers to the number of monthly-box-means with $n \geq 10$ on both cloudy**
585 **and clear cases.**

586

587

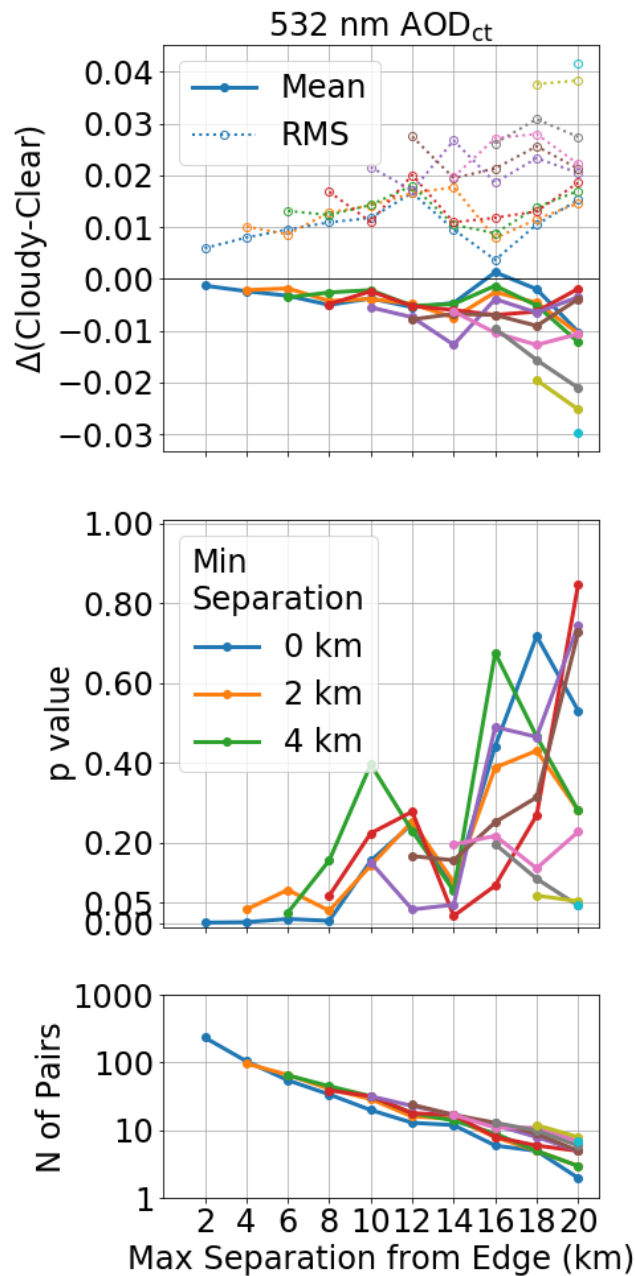
588

589



590 **Figure 5. (a) The local-scale near-synchronous samples of the AOD above cloud top height.**
 591 **Each marker represents the mean over the cloudy and clear sides of a cloud edge, each 2-6**
 592 **km from the edge. The bars indicate the standard deviation of the measurements in each**
 593 **side, almost all of them too short to be discernible. (b) Same as (a) except for the horizontal**
 594 **separation of 4-12 km.**

596
 597
 598



599

600 **Figure 6. (a) The mean and root-mean-square deviations of the AOD above cloud top**
 601 **between the cloudy and clear sides of cloud edges. Each side is defined by the horizontal**
 602 **separation from cloud edge. The maximum separation (e.g., 12 km in Fig. 3) is indicated on**
 603 **the x axis. Each line represents the minimum temporal separation (e.g., 4 km in Fig. 3) of 0,**
 604 **2, 4, ..., 18 km in descending order of line length. (b) The p values determined through the**
 605 **paired t-test. (c) the number of cloudy/clear pairs.**